Progressive Generation of Control Frameworks for Image Registration

Liang-Chien Chen and *Liang-Hwei Lee*
Center for Space and Remote Sensing Research, National Central University, Chung-Li, Taiwan 320, Republic of China

ABSTRACT: An original scheme to automatically generate control point pairs for image registration in a progressive way is presented here. It consists of three stages of processing. In the first stage, the Voronoi-Delaunay dual graph is used to predict the optimal location for a new control point to be generated. Second, a target-defined interest operator is designed to extract feature points from the predicted area. In the third stage, a hierarchical templet matching procedure is applied. A global consistency check by robust estimation to improve its reliability is also included. The major features of the proposed scheme are that (1) it yields highly reliable and accurate results, (2) the distribution of generated control points is uniform, and (3) it is computationally efficient. Examples illustrating the operation of the scheme are presented.

INTRODUCTION

THE REGISTRATION BETWEEN A REFERENCE IMAGE and its counterpart, a second remotely sensed image, is a necessity in many image analysis tasks such as change detection (Swain, 1985), feature or color enhancement (Carper *et al.*, 1990; Ehlers *et al.*, 1990), three-dimensional (3D) reconstruction (Greenfeld and Schenk, 1989), and map revision (Swann *et al.*, 1988). The procedure of image registration may be divided into two steps. The first is to select enough registration control points (RCPs) with a suitable distribution and then to measure the corresponding image coordinates. The second step is to choose a mapping function after which a coordinate transformation is performed followed by image resampling. The second step is straightforward. However, the first step relies on a manual operation which is labor intensive and time consuming.

To overcome these drawbacks, several approaches striving to automate the procedure have been proposed. Stockman *et al.* (1982) extracted feature lines and then utilized their endpoints or line crossings as RCPs. Goshtasby *et al.* (1986) segmented feature polygons, lakes for instance, then calculated the centers of gravity as RCPs. Ton and Jain (1989) improved Goshtasby's method by a relaxation matching algorithm. Nevatia and Medioni (1984) matched feature lines according to their graphic structure. All of the stated approaches, which either used the relaxation method or utilized the graphic relationship of a convex hull to determine the RCP's correspondence, are computationally intensive. More importantly, these approaches suffer from the following limitations: (1) the number of RCPs is often not sufficient due to the feature line extraction procedure, (2) the distribution of RCPs is not always uniform, and (3) the point-to-point correspondence is not always sufficiently accurate. Accordingly, we propose a scheme which can efficiently generate large enough amounts of RCP pairs with a uniform distribution at sub-pixel accuracy. The flow chart of the scheme is shown in Figure 1.

GENERATION FOR UNIFORMLY DISTRIBUTED POINTS

The Voronoi-Delaunay dual diagram has been widely used in computer graphics (De Floriani *et al.*, 1989), vision (Ahuja and Tuceryan, 1989), and surface modeling (Gold, 1988). The diagram is constructed from a group of existing points on a plane or in space. We, from another point of view, use the diagram to predict the optimal location for a new point to be generated. The Delaunay triangulation has the property of equiangularity. This means that the triangulation should satisfy the Max-Min Angle Criterion which is completely equivalent to the Circle Criterion (Lawson, 1977).
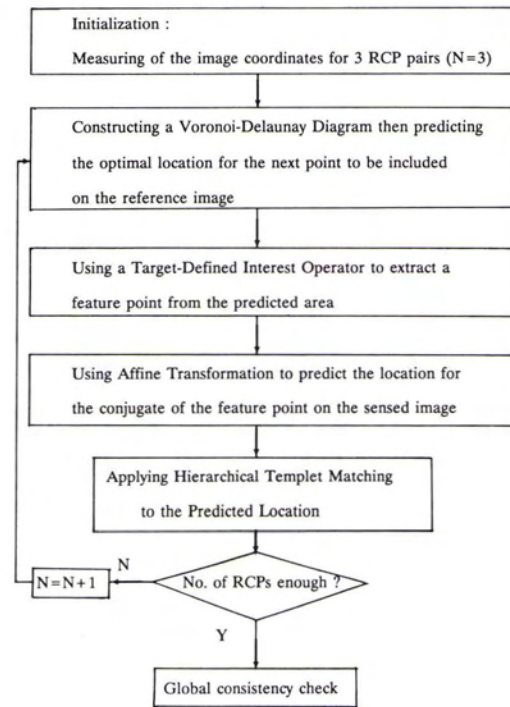

FIG. 1. Flow chart of the proposed scheme.

There are two algorithms used to construct a Delaunay triangulation (Lee and Schachter, 1980). The first is the Divide-and-Conquer (DAC) method. The method is efficient in computation; however, it considers all of the points simultaneously so is rather involved. The second algorithm is called the Local Optimization Procedure (LOP) which, based on the circle criterion and point-by-point processing, is simpler to understand and simpler to program. Referring to Figure 2, the procedure of the LOP given by Lawson (1977) and Lee and Schachter (1980) is briefly stated as follows.

Let e be an internal edge of a triangulation and R be the quadrilateral $P_1 P_2 P_3 Q$ formed by the two triangles $P_1 P_2 P_3$ and $P_1 P_3 Q$ having e as their common edge. Consider the circumcircle of one of the triangles. This circle passes through three vertices, P_1, P_2, and P_3, of R. If the fourth vertex, Q, of R is within the circle, replace e by the other diagonal of R, i.e., connecting $P_2 Q$ and deleting e. Otherwise triangles $P_1 P_2 P_3$ and $P_1 P_3 Q$ are

kept without swapping the common edge e. We have two major reasons to use LOP in this investigation: (1) our scheme generates one point at a time and LOP is a point-by-point procedure, so LOP is more suitable than DAC due to procedural similarity; and (2) the triangulation only needs to be reconstructed locally when a new point is included.

A Voronoi point is the center of the circumcircle for the associated Delaunay triangle. The triangle is the one out of a Delaunay triangulation which satisfies the property of equiangularity. That means the triangles in the triangulation are as equiangular as possible, so as to avoid thin and long triangles. The basic idea of our approach to locate the optimal position for a new RCP is to select the Voronoi point when the associated Delaunay triangle has the largest circumcircle. Accordingly, the triangle with the largest circumcircle in the triangulation is always targeted for a new point generation. This implies that the diameter of the largest circumcircle is minimized. Hence, the uniform distribution for the RCPs is always maintained. The procedure is stated as follows:

(1) Construct a Delaunay triangulated network from existing RCPs and boundary corners by using the LOP.
(2) Construct the Voronoi diagram for the points within the area of interest.
(3) Clip out the Voronoi polygons which are outside the area of interest; then the intersections between the Voronoi polygons and the boundary are treated as Voronoi points.
(4) Calculate the distances between each RCP and the surrounding vertices of the Voronoi polygon, then search for the local maximum Ld:
Let S be the set of m vertices of a Voronoi polygon associated with point P; i.e.,
$$S = \{Q_k / Q_k = (x_k, {}_yk)\}\ k = 1,2,...,m,$$
then $Ld_i = \max \{d_k / d_k = \overline{PP_k}\}\ k = 1,2,...,m.$
(5) Search for the global maximum from Lds; i.e.,
$$Gd = \max \{Ld_i\}\ i = 1,2,...,n.$$
(6) The point with Gd is the newly predicted RCP.

Figure 3 illustrates the procedure, from (a) to (f), for point densification, where the solid lines form the Delaunay triangulation and the dashed lines in (b) are the Voronoi polygons. Starting from point 1,2, and 3, Figure 4(a) shows the triangulation structure when 50 new points are generated. Figure 4(b) shows the triangulation when the boundary is an arbitrarily shaped convex hull.

EXTRACTION FOR FEATURE POINTS

A feature point which can be extracted with an interest operator is described by its high variance or steep gradients with its surroundings (Förstner, 1987). Due to its limitation to a local extension, feature points lack geometric attributes or high level symbolic features when compared to line or polygon features. However, a point is geometrically and projectively invariant. Accordingly, taking advantage of this attractive property under the geometric constraint whi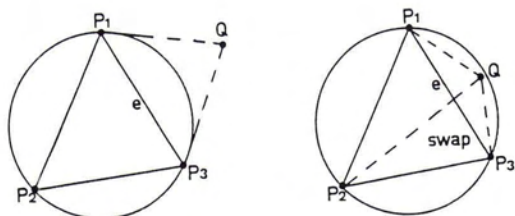ch is derived from the prediction procedure stated in the last section, feature points are used for successive matching in this investigation.

Several interest operators have been proposed (Moravec, 1977; Luhmann and Altrogge, 1986; Förstner and Gulch, 1987; Lü, 1988). Lü's model is most efficiently computed; however, it extracts a few points from a diagonal feature line. This behavior often makes successive templet matching unreliable. To alleviate this problem, we shall propose a target-defined ground operator (TDGO) to screen an image first followed by feature point extraction.

TDGO

A bit pattern with a 3 by 3 window is used for topological encoding. According to Figure 5, the code for a surrounding point i of center o is computed as

$$IF\ |G_o - G_i| > \delta \quad Then\ B_i = 2^{i-1}$$
$$Else\ B_i = 0,$$
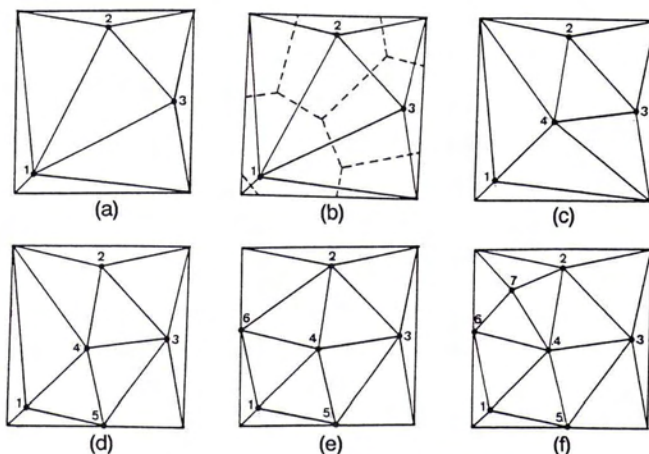$$for\ i = 1, 2, ... , 8,$$

where

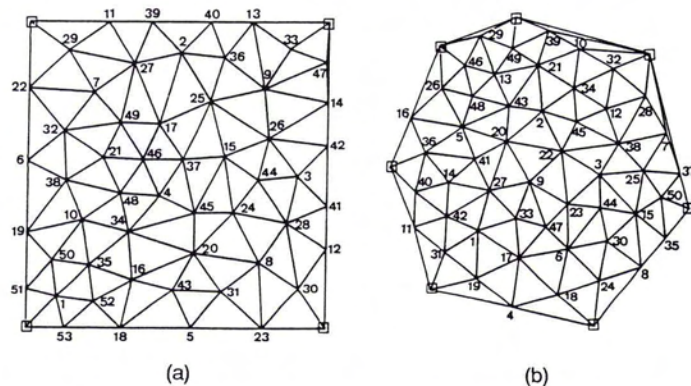FIG. 3. The densification procedure.

FIG. 4. Delaunay triangulation of generated points in a/an. (a) Square boundary. (b) Arbitrarily shaped convex boundary.

7	8	1		6 4	128	1
6	0	2		3 2	×	2
5	4	3		1 6	8	4

(a)   (b)

FIG. 5. Bit pattern (a) and position codes (b).

FIG. 2. Local optimization procedure (based on the circle criterion).

G_o = grey value of the center o,
G_i = grey value of the surrounding pixels,
δ = threshold, and
B_i = position code.

Thus, the bit value BV is

$$\text{BV} = \sum_{i=1}^{8} B_i$$

A look-up table is built for fast processing. The 24 selected patterns and the associated BVs are shown in Figure 6. By visually examining the figure, one will see that each selected pattern has a 90° angle at the center. Hence, after screening by TDGO, only right-angled corner points, which are potentially good feature points, are retained.

INTEREST VALUE

After sieving with TDGO, the quantity of points to be processed at this stage is significantly reduced. Then the interest value, IV, is calculated as

$$\text{IV} = \sum_{i=1}^{8} |G_o - G_i|$$

After suppression of the local non-maximum for IVs (Lü, 1988) in the area of interest, interest points are thus selected. To keep the procedure flexible in the following templet matching, we retain up to five points as candidates. The point with the largest IV is used first for successive matching. If the matching is successful, the RCP pair is determined. If not, the point with the second largest IV is processed and so forth. If none of the five candidates is successfully matched, the point with the largest IV is marked without searching for its corresponding point. Thus, the procedure returns to the prediction model for the next point by using the Delaunay-Voronoi diagram.

HIERARCHICAL TEMPLET MATCHING

Once an interest point is extracted from the reference image, the location of its corresponding point on the sensed image is predicted by affine transformation based on the existing RCP pairs (Förstner, 1987). The next step is to perform the similarity assessment by hierarchical templet matching.

ADJACENT PIXEL DIFFERENCE METHOD

In the similarity assessment, the Adjacent Pixel Difference (APD) method (Satishchandra, 1982) is applied. The APD method accesses the similarity between two image patches according to the row and column feature vectors which are derived by normalizing the sum of grey value differences between two consecutive row pixels and column pixels, respectively. It was found that the APD is computed quickly and yields accurate enough matching as initial image coordinates for target and search windows for successive least squares fine matching. Thus, APD is integrated into our scheme. APD uses the 2- by M-pixel long feature vectors, which are derived from a 2D window with M by M pixels, to calculate the correlation coefficients. The feature vector of a target window with M by M pixels is

$$\mathbf{f}_m^r = [R_1, R_2, ..., R_m, C_1, C_2, ..., C_m]$$

where the row feature vector $\mathbf{R}_l$ and the column feature vector $\mathbf{C}_s$ are computed respectively as

$$\mathbf{R}_l = \left[\sum_{y=1}^{m-1} |I(l,y) - I(l,y+1)|\right] \bigg/ \sum_{y=1}^{m} I(l,y),$$

where $l = 1, 2, ..., m$, and

$$\mathbf{C}_s = \left[\sum_{x=1}^{m-1} |I(x,s) - I(x+1,s)|\right] \bigg/ \sum_{x=1}^{m} I(x,s),$$

where $s = 1, 2, ..., m$.

The feature vector for a search window $\mathbf{f}_{i,j}$ is derived in the same manner. Thus, the best matched pixel (i^*, j^*) in the search area is defined by having the largest correlation coefficients $C_{i,j}$ where

$$C_{i,j} = \frac{\mathbf{f}_m^r \cdot \mathbf{f}_{i,j}}{\|\mathbf{f}_m\| \, \|\mathbf{f}_{i,j}\|}.$$

QUAD-TREE HIERARCHY

A quad-tree structure is used to represent the hierarchy among layers in the matching procedure. The resolution between two consecutive layers is reduced by two as shown in Figure 7(a). Let the matched position in a coarse layer of a search window be (i^*, j^*), and the possible corresponding pixels in the finer layer, illustrated in Figure 7(b), be $(2i^*, 2j^*)$, $(2i^*+1, 2j^*)$, $(2i^*, 2j^*+1)$, and $(2i^*+1, 2j^*+1)$. Thus, the similarity assessment only needs to apply to those four pixels. This hierarchical matching is performed layer by layer sequentially from coarse to fine and stops when the matching for the finest layer is accomplished.

LEAST-SQUARES FINE MATCHING

It has been demonstrated that least-squares matching (LSM) can potentially achieve an accuracy up to 0.05 pixels for images with good texture (Ackermann, 1984). Due to its high accuracy, LSM is widely used in digital photogrammetric tasks such as image coordinate measurements and automated DTM generation (Helava, 1988; Rosenholm, 1986). LSM is suitable for our final matching refinement because the feature points which we extracted have excellent textural information. Moreover, we found out that the APD can reach a matching accuracy of 1 to 2 pixels which is good enough to provide the initial value for LSM.
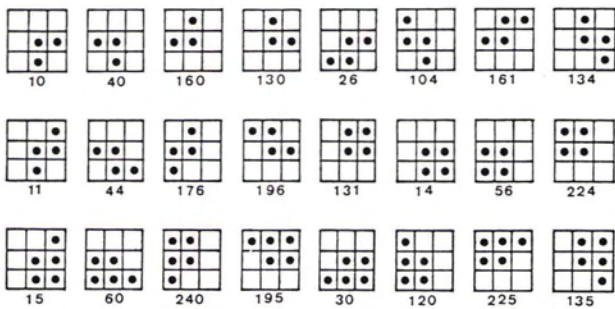
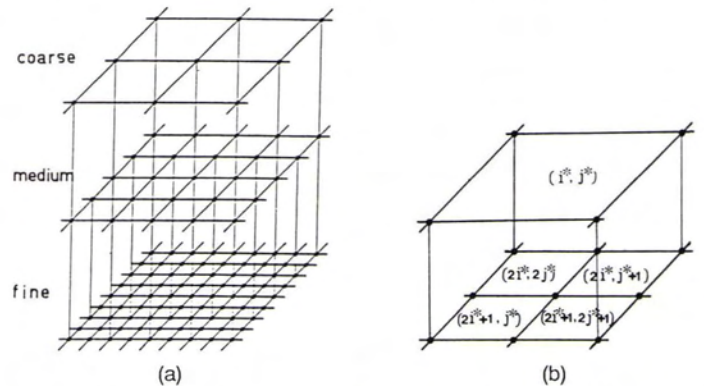

FIG. 6. Selected patterns and bit values.

FIG. 7. Coarse-to-fine hierarchy. (a) Structure. (b) Pixel correspondence.

The LSM is used to determine the conjugate correspondence which minimizes the sum of the squares for grey value differences. Considering the geometric deformation, the following condition should be satisfied:

$$G_1(x, y) = G_o + S * G_2(x, y; \mathbf{A})$$

where G_1 and G_2 are the grey values for the target and search windows, respectively;

G_o and S are respectively the shift and scale for the grey values; and

$\mathbf{A}$ is the affine coefficient matrix.

If the geometric deformation is not encountered, $\mathbf{A}$ is a unit matrix and the scaling factor is equal to one.

GLOBAL CONSISTENCY CHECK

To improve the reliability and accuracy of the registration, a global consistency check is needed after the whole matching procedure is finished. The consistency check is performed by robust estimation when a mapping function between a reference image and its counterpart is given. The selection for a mapping function between an image and its counterpart should consider their geometrical properties. In this investigation, we select the affine transformation (ASP, 1983) for satellite images and the coplanarity condition (ASP, 1980) for a stereo pair of aerial photographs. The robust estimation is a weighting procedure for the observations. The weight for a potential blunder is relaxed with each iteration to reduce the influence on the solution. Accordingly, the residual for a blunder increases as the weight is reduced in each iteration. Thus, the blunder is localized. The weighting function with some empirical values for a potential blunder used in this investigation is

$$P = \begin{cases} 1 & \text{when } |v| < 2\sigma_o, \\ \exp\left[-0.05\left(\frac{|v|^{4.4}}{\sigma_o}\right)\right] & \text{for the first three iterations when } |v| > 2\sigma_o, \\ \exp\left[-0.05\left(\frac{|v|^{3.0}}{\sigma_o}\right)\right] & \text{for the fourth iteration and afterwards.} \end{cases}$$

EXPERIMENTAL RESULTS

The experiment includes tests of image-to-image registration for

- three pairs of SPOT multi-temporal red band scenes in the multispectral mode,
- a SPOT panchromatic scene and a red band scene in the multispectral mode, and
- a stereo pair of aerial photographs.

All of the images were acquired from the Image Data Base of Taiwan (Fu, 1987). The window size for extracting interest points is 27 by 27 pixels. The size of the target window in pixels in hierarchical templet matching varies from 64 by 64 to 16 by 16. The window size for the LSM is 21 by 21 pixels. The minimum requirement of the normalized cross correlation coefficient for a successful match is 0.8. The maximum number of iterations for the LSM is 30. The mapping function for satellite imagery in a consistency check is the affine transformation. For aerial photographs, the mapping function is the coplanarity condition. For satellite images and aerial photographs, the initialization for RCP positions can be further automated rather than using only manual measuring as shown in Figure 1. The method for doing so is to give approximate locations for three pairs of RCPs according to the rough estimates of image shifts in rows and columns. Then feature point extraction and hierarchical matching are carried out to determine the precise correspondences for three RCP pairs.

CASE I

The basic descriptions for three red-band SPOT images are shown in Table 1.

Figure 8(a) is the reference image, SPC 019, when SPC 055 as shown in Figure 8(b) is registered. In both Figures 8(a) and 8(b), the square marks show the locations for 50 RCPs which are automaticablly generated. Figure 8(c) illustrates the Delaunay triangulation constructed from the 50 RCPs on SPC 019. Figure 8(d) is the local enlargement showing the RCPs in detail. Figures 8(e) and 8(f) show the registration between SPC 019 and SPC 092. Figure 8(g) is the site map in which major roads and a river are illustrated. Due to the limitations of the map scale and the image resolution, it is difficult to identify the roads on the image. However, one can easily recognize the generated RCPs in terms of the image features in the local enlargement of Figure 8(d). Figure 8(h) shows the vectors of the registration error between SPC 019 and SPC 055. Similarily, Figures 8(i) and 8(j) show the vectors of registration error between SPC 019 and SPC 092 and between SPC 055 and SPC 092, respectively. The accuracy analysis for the registration is summarized in Table 2 where the least-squares matching includes LSM-1, which is not considered a geometric deformation between images, and LSM-2 which is otherwise. The RMSE is between 0.17 pixels to 0.27 pixels.

CASE II

The registration between two SPOT images with different ground resolutions is investigated in this case. The parameters of these images are described in Table 3. SPC 074, shown in Figure 9(a), is a SPOT panchromatic image with 10-m resolution and is treated as a reference. On the other hand, the sensed image is the red band of SPC 075 which is in SPOT multispectral mode with 20-m ground resolution. The sensed image after magnification by 2 is shown in Figure 9(b). The automatically generated RCPs are also marked in both Figures 9(a) and 9(b). Figure 9(c) is the site map in which contour lines, major roads,

TABLE 1. PARAMETERS FOR THREE SPOT RED BAND IMAGES

Scene ID	Sampling Date	Incidence	Resolution/Level
SPC 019	04/10/86'	R 24.1°	20m/1B
SPC 055	13/10/87'	R 09.7°	20m/1B
SPC 092	07/12/88'	vertical	20m/1B

TABLE 2. ACCURACY ANALYSIS IN CASE I

Scene ID	Fine Matching Method	Ratio of Matched Points	No. of Reliable RCPs	Max. Error (Pixel) Line	Max. Error (Pixel) Sample	RMSE (Pixel)
SPC 019/SPC 055	LSM-1	55/57	50	0.60	0.43	0.17
	LSM-2	55/57	50	0.46	0.51	0.20
SPC 019/SPC 092	LSM-1	52/57	48	0.87	0.99	0.26
	LSM-2	52/57	48	0.54	0.68	0.27
SPC 055/SPC 092	LSM-1	54/57	51	0.62	0.71	0.23
	LSM-2	54/57	51	0.71	0.68	0.27

TABLE 3. PARAMETERS FOR 2 SPOT IMAGES

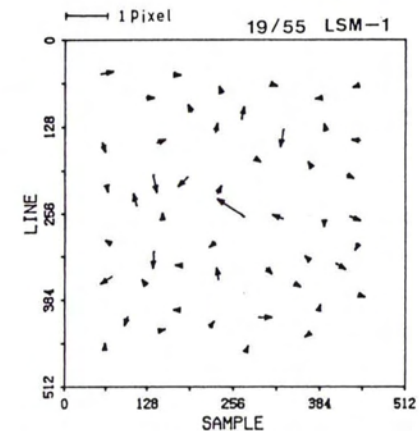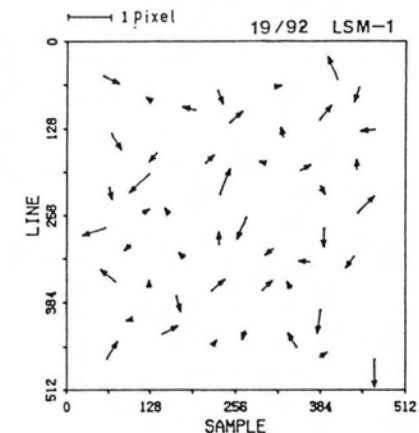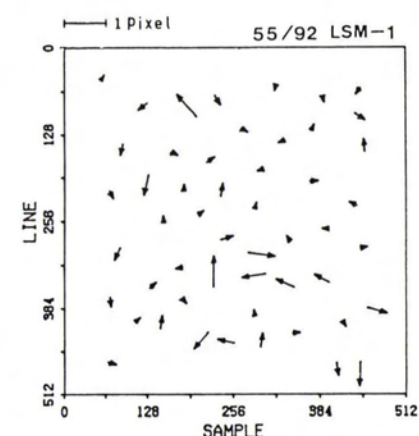| Scene ID	Sampling Date	Incidence	Resolution/Level
SPC 074	15/01/88'	R 19.9°	10m/1B
SPC 075	15/01/88'	R 19.9°	20m/1B
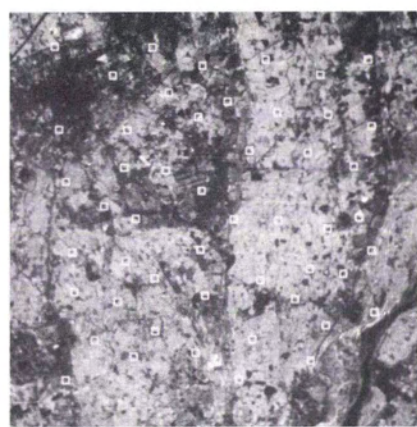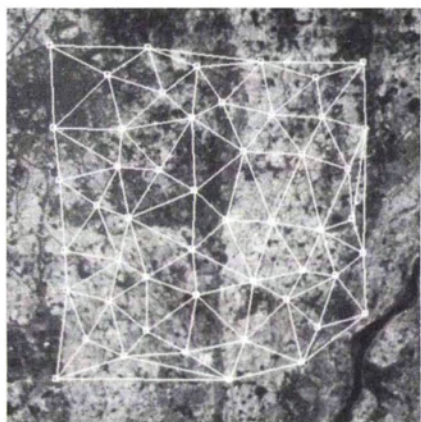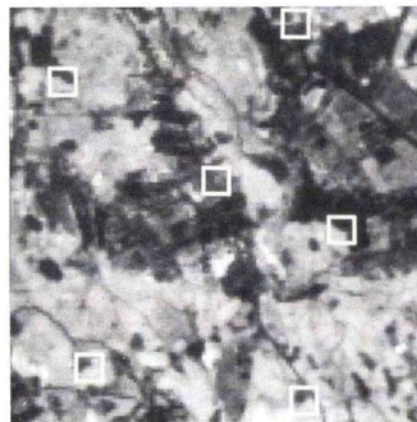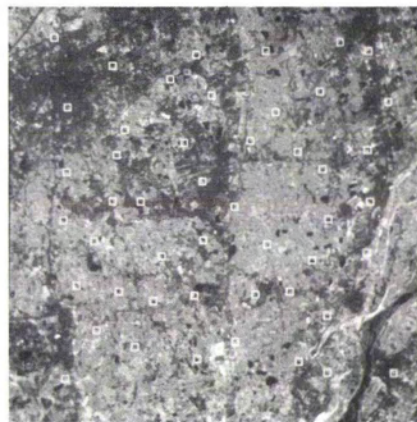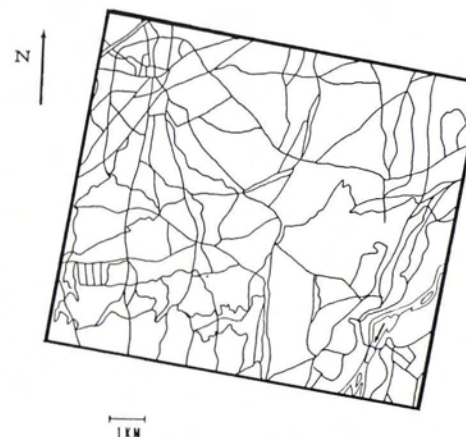
FIG. 8. (a), (b) SPC 019 and SPC 055 with RCP pairs. (c) Delaunay triangulation on SPC 019. (d) Local enlargement of SPC 019. (e), (f) SPC 019 and SPC 092 with RCP pairs. (g) The site map. (h), (i), (j) Error vectors. (© SPOT Image Corp., copyright 1986, 1987, and 1988, CNES.)
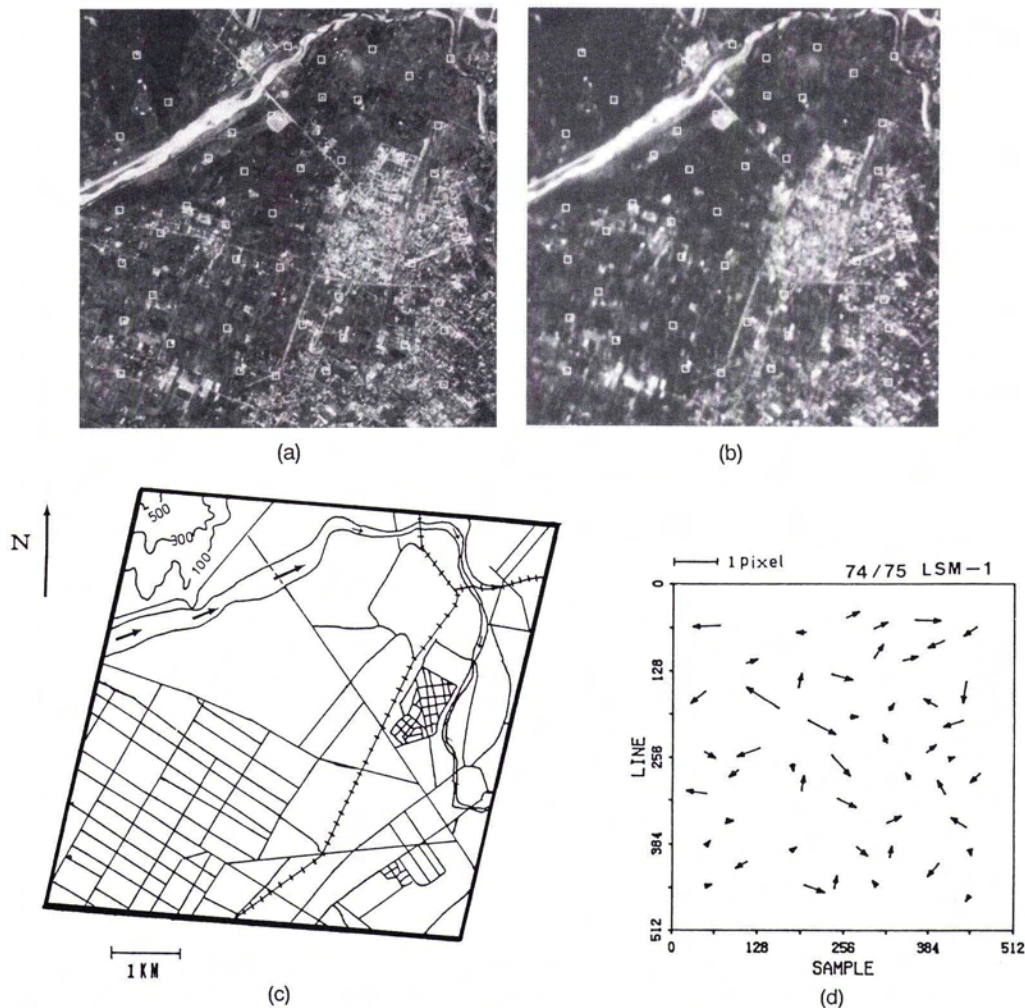
FIG. 9. (a) SPC 074. (b) SPC 075 (red band, magnified by 2). (c) The site map. (d) Error vectors. (© SPOT Image Corp., copyright 1988, CNES.)

railroads, and a river are illustrated. Figure 9(d) shows the vectors of the registration error. The registration accuracy analysis is presented in Table 4. The RMSE is 0.27 pixels under 10-m resolution.

CASE III

A stereopair of aerial photographs, ID3741 and ID3745, is tested in this example. Each of the standard 9- by 9-inch aerial photographs is scanned with an EIKONIX 1412 to 4,096 by 4,096 pixels. The images are then reduced by simple averaging of non-overlapping sets of 4 by 4 pixels to 1,024 by 1,024 pixels as shown in Figures 10(a) and 10(b). Figure 10(c) is the site map for the stereo pair in which contour lines and major roads are illustrated. Figure 10(d) shows the vectors of the y-parallax after relative orientation modeling using the coplanarity condition. The registration accuracy is described in Table 5. The RMS of the y-parallax is 0.14 pixels.

SUMMARY OF THE EXPERIMENTAL RESULTS

- The registration error for multi-temporal SPOT images reaches 0.17 pixels.
- The registration error for a SPOT multispectral image on a panchromatic scene under 10-m ground resolution is 0.27 pixels.
- The y-parallax for a pair of aerial photographs is 0.14 pixels using the proposed method.

TABLE 4.　ACCURACY ANALYSIS IN CASE II

Scene ID	Fine Matching Method	Ratio of Matched Points	No. of Reliable RCPs	Max. Error (Pixel) Line	Sample	RMSE (Pixel)
SPC 074/SPC 075	LSM-1	53/57	49	0.75	0.50	0.28
	LSM-2	53/57	49	0.64	0.40	0.27

- The whole processing time for generating a new point is about 6 seconds when a PC/AT 386-25 and an 80387 coprocessor is used.
- By the use of visual inspection, the uniform distribution for generated RCPs is successfully maintained. The ratio between the maximum diameter of the circumcircle for the Delaunay triangulation and the minimum one is tested to quantitatively demonstrate the uniformity. The ratio ranges from 1.5 to 1.7 in all cases.
- The method can generate a sufficient number of RCPs provided enough point features are available.

CONCLUSIONS

The proposed method overcomes the drawbacks which current methods have encountered as described in the Introduction and satisfies the requirements with high accuracy, high computational efficiency, and uniform distribution for the RCPs. Many image-to-image registration related tasks, e.g., change detection, feature or color enhancement, 3D reconstruction, and map
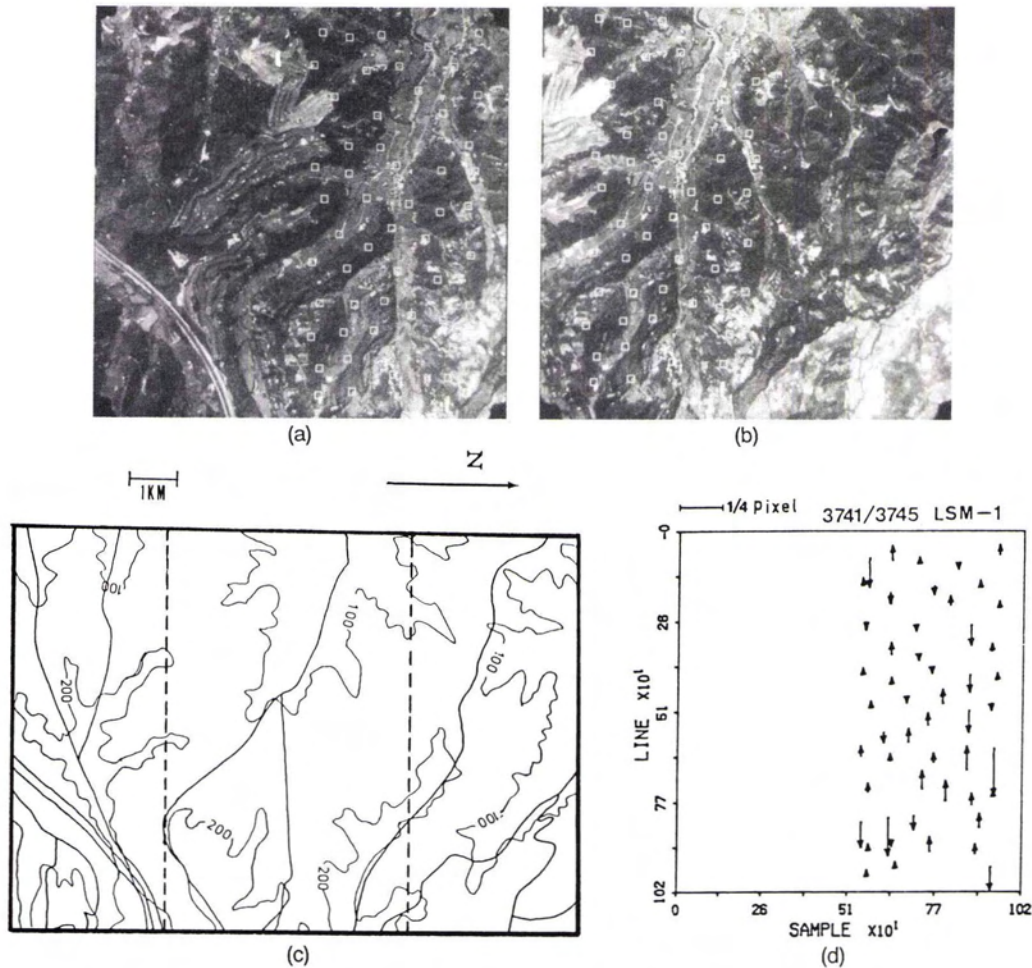
FIG. 10. (a) ID 3741. (b) ID 3745. (c) The site map. (d) Vectors of the y-parallax.

TABLE 5. ACCURACY ANALYSIS IN CASE III

Scene ID	Fine Matching Method	Ratio of Matched Points	No. of Reliable RCPs	Max. Y-Parallax (Pixel)	RMSE Y-Parallax (Pixel)
3741/3745	LSM-1	57/57	53	0.43	0.14
	LSM-2	57/57	53	0.33	0.14
	LSM-1	106/107	99	0.38	0.14
	LSM-2	106/107	99	0.31	0.14

revision, can thus be made more efficient and automatic by using this method. The method is applicable to SPOT images and digitized aerial photographs. The applicability of the method to Landsat images is quite promising because the geometric deformation of the images is relatively small due to their nadir scanning and small field of view. On the other hand, the registration for images from Synthetic Aperture Radars, low attitude airborne multispectral scanners, or close-range photography needs further investigation. The accuracy evaluation for the method would be more reasonable by considering relief displacement and using a DTM for a mountainous area.

REFERENCES

Ackermann, F., 1984. Digital Image Correlation: Performance and Potential Application in Photogrammetry. *Photogrammetric Record*, 11(64):429-439.

Ahuja, N., and M. Tuceryan, 1989. Extraction of Early Perceptual Structure in Dot Pattern : Integrating Region, Boundary, and Component Gestalt. *Computer Vision, Graphics, and Image Processing*. 48(3):304-356.

American Society of Photogrammetry, 1983. *Manual of Remote Sensing, Second Edition*. ASP, Falls Church, Virginia, 2440 p.

——, 1980. *Manual of Photogrammetry, Fourth Edition*. ASP, Falls Church, Virginia, 1056 p.

Carper, W., T. Lillesand, and R. Kiefer, 1990. The Use of Intensity-Hue-Saturation Transformation for Merging Panchromatic and Multispectral Image Data. *Photogrammetric Engineering & Remote Sensing*, 56(4):459-467.

De Floriani, L., B. Falcidieno, and C. Pienovi, 1985. Delaunay-Based Representation of Surfaces Defined over Arbitrarily Domains. *Computer Vision, Graphics, and Image Processing*, 32(1):127-140,

——, 1989. Structured Graph Representation of a Hierarchical Triangulation. *Computer Vision, Graphics, and Image Processing*, 45(2):215-226.

Ehlers, M., M. Jadkowski, R. Howard, and D. Brostuen, 1990. Application of SPOT Data for Regional Growth Analysis and Local Planning. *Photogrammetric Engineering & Remote Sensing*, 56(2):175-180.

Förstner, W., and E. Gulch, 1987. A Fast Operator for Detection and Precise Location of Distinct Points, Corners and Centers of Circular Features. *Intercommission Conference on Fast Processing of Photogrammetric Data*. Interlaken, Switzerland, pp. 281-305.

Fu, A. -M., 1987. The Establishment of the Base Map System and Its Applications. *The Journal of Chinese Society of Photogrammetry and Remote Sensing*, No.12, pp. 1-64 (in Chinese).

Gold, C., 1988. *Point and Area Interpolation and the Digital Terrain Model.* University of New Brunswick Technical Report No. 136, pp. 133-147.

Goshtasby, A., G. Stockman, and C. Page, 1986. A Region-Based Approach to Digital Image Registration with Subpixel Accuracy. *IEEE Transactions on Geoscience and Remote Sensing,* GE-24(3):390-399.

Greenfeld, J., and A. Schenk, 1989. Experiments with Edge-Based Stereo Matching. *Photogrammetric Engineering & Remote Sensing,* 55(12):1771-1777.

Helava, U., 1988. Digital Comparator Correlator System. *International Archives of Photogrammetry and Remote Sensing,* Kyoto, Japan, 27(2):160-170.

Lawson, C., 1977. *Software for C Surface Interpolation. Mathematical Software III* (J. Rice, ed.), Academic Press, New York, N. Y., pp.161-194.

Lee, D., and B. Schachter, 1980. Two Algorithms for Constructing a Delaunay Triangulation. *International Journal of Computer and Information Science,* 9(3):219-242.

Lü, Y., 1988. Interest Operator and Fast Implementation. *International Archives of Photogrammetry and Remote Sensing,* Kyoto, Japan, 27(3):491-500.

Luhmann, T., and G. Altrogge, 1986. Interest Operator for Image Matching. *International Archives of Photogrammetry and Remote Sensing,* Ravaniemi, Finland, 26(3):459-474.

Moravec, H., 1977. Towards Automatic Visual Obstacle Avoidance. *International Joint Conference of Artificial Intelligence,* Tokyo, Japan, p. 584.

Nevatia, R., and G. Medioni, 1984. Matching Images Using Linear Features. *IEEE Transactions on Pattern Analysis and Machine Intelligence,* PAMI 6(6):675-685.

Rosenholm, D., 1986. Accuracy Improvement of Digital Matching for Evaluation of Digital Terrain Models. *International Archives of Photogrammetry and Remote Sensing,* Rovaniemi, Finland, 26(3):573-587.

Satishchandra, D., J. Boland, H. Ranganath, and W. Malcom, 1982. Multiple Image Registration Using Feature Based Adjacent Pixel Difference. *IEEE Computer Society Conference on Pattern Recognition and Image Processing,* pp.524-529.

Stockman, G., S. Kopstein, and S. Benett, 1982. Matching Images to Models for Registration and Object Detection via Clustering. *IEEE Transactions on Pattern Analysis and Machine Intelligence,* PAMI-4(3):229-241.

Swain, P., 1985. Advanced Interpretation Techniques for Earth Data Information System. *Proceedings of IEEE,* 73(6):1031-1039.

Swann, R., D. Hawkins, A. Westwell-Roper, and W. Johnstone, 1988. The Potential for Automated Mapping from Geocoded Digital Image Data. *Photogrammetric Engineering & Remote Sensing,* 54(2):187-193.

Ton, J., and A. Jain, 1989. Registering Landsat Images by Point Matching. *IEEE Transactions on Geoscience and Remote Sensing,* GE-27(5):642-651.

LIST OF "LOST" CERTIFIED PHOTOGRAMMETRISTS

We no longer have valid addresses for the following Certified Photogrammetrists. If you know the whereabouts of any of the persons on this list, please contact ASPRS headquarters so we can update their records and keep them informed of all the changes in the Certification Program. Thank you.

Robert Ball	P.L. Grant	Wesley Norris
Milosh Benesh	William Grehn	Frank Pabian
Ivan Bentley	David Gustafson	Gene A. Pearl
Binisain Bhawani	Jack Guth	Jay Paik
Dewayne Blackburn	Elwood Haynes	John Price
Gerard Borsje	F.A. Hildebrand, Jr.	Larry Reed
Edward Brandenberg	James Hogan	Sherman Rosen
William Brown	Clyde Hubbard	Carl Schafer
Eugene Caudell	Daniel Hughes	Lane Schultz
William Clements	Lawrence James	Charles Sheaffer
Robert Denny	William Janssen	Leo Strack
Russell Doolittle	Harold Johnson	Gelacio Sumagaysay
Leo Ferran	Lawrence Johnson	Wallie Swain
Jimmie Felton	Spero Kapelas	Keith Syrett
Charles Foster	Andre Langevin	William Taylor
Christopher Foster	Scott Lovern	William Thomasset
Stanley Frederick	Andrew Martin	Conrad Toledo
Robert Fuoco	William McKeague	Raymond Town
Franek Gajdeczka	Francisco Milande	Robert Tracy
George Gajate	Marinus Moojen	Peter Warneck
George Glaser	Philip Mulvey	Lawrence Watson
Jose Gotay	W. S. Niesen	Randal Weltzin